ELSEVIER

International Journal of Mass Spectrometry 192 (1999) 379–386

International Journal of Mass Spectrometry

Laser control of molecular ionization with intense short laser pulses

André D. Bandrauk*, Heng Tai Yu

Laboratoire de Chimie Théorique, Faculté des Sciences, Université de Sherbrooke, Sherbrooke, Quebec J1K 2R1, Canada

Received 9 December 1999; accepted 18 May 1999

Abstract

Numerical solutions of the time-dependent Schroedinger equation of the two molecules H_2^+ and H_2 allow for nonperturbative calculations of ionization rates in short intense laser pulses ($\tau < 1$ ps, $I \simeq 10^{14}$ W/cm^2). It is shown that the coherent superposition of two pulses of frequency ω and 2ω results in optimal control of the ionization process at critical internuclear distances R_c where charge resonance enhanced ionization (CREI) occurs. The implications of CREI are discussed for laser control of ionization in mass spectrometry. (Int J Mass Spectrom 192 (1999) 379–386) © 1999 Elsevier Science B.V.

Keywords: Laser control; Coherent control; Charge resonance ionization; Time-dependent Schroedinger equation; Intense short laser pulses; Laser mass spectrometry

1. Introduction

The advent of short ($\tau < 1$ ps), intense ($I > 10^{14}$ W/cm^2) laser pulses has led to investigations of the regime of nonlinear, nonperturbative laser–matter interaction. The atomic case is now well documented in a recent review [1] that emphasizes the discovery of new nonlinear multiphoton process such as above threshold ionization (ATI) and high order harmonic generation. Much of the physics of atom–laser interaction in the high intensity, low frequency regime can be readily understood in terms of a quasistatic model and plasma physics concepts [2–4].

The behaviour of molecules in intense laser fields offers a new challenge due to the presence of the nuclear degrees of freedom [5]. Thus using the dressed molecule picture it was predicted earlier that new laser-induced bound states could be created by laser induced avoided crossings between molecular states below ionization thresholds [5–8]. These states have now been experimentally confirmed [9]. With current high intensities approaching the atomic unit of field ($\mathcal{E}_0 = e^2/a_0^2 = 5 \times 10^9$ V/cm) and the corresponding intensity ($I_0 = c\mathcal{E}_0^2/8\pi = 3 \times 10^{16}$ W/cm^2), ionization is a dominant process. It has been shown recently by three-dimensional (3D) numerical simulations that intense laser-field ionization of a molecular ion is dramatically different from an atomic system. Thus in both the one-electron molecular ions H_2^+ [10,11] and H_3^{2+} [12] for which the first accurate full quantum 3D Born-Oppenheimer ionization rate calculations have been performed for linearly polarized light parallel to the linear molecular orientation, it was found that ionization rates exceed that of the H

* Corresponding author. E-mail: andre.bandrauk@courrier.uscherb.ca

PII S1387-3806(99)00114-1

atoms by at least one order of magnitude and reach a maximum at critical distance R_c for linear molecules and also at critical angles θ_c for nonlinear systems [13]. This laser-induced molecular enhancement of ionization rates can be attributed to overbarrier ionization of the lowest unoccupied molecular orbital (LUMO) that is populated and displaced upwards by the Stark effect of the instantaneous laser field E at its peak. Thus, the quasistatic field model, as earlier suggested by Codling et al. [14] can be used to rationalize molecular ionization rates and this has been confirmed now by many numerical simulations in the Born-Oppenheimer approximation (fixed nuclei) [10–13], [15] and the first exact non-Born-Oppenheimer calculations with moving nuclei [16,17]. We have derived in previous work analytic expressions for the critical distance, $R_c = 4/I_p$ in H_2^+ [18] and $R_c = 5/I_p$ in H_3^{2+} [19] based on a CREI model where I_p is the ionization potential of the neutral atom, and have shown it to be relatively independent of nuclear charge and field strength around intensities $I = 10^{14}$ W/cm^2. We have called this ionization enhancement effect charge resonance enhanced ionization (CREI) as it depends on a fundamental molecular spectroscopic phenomenon, charge resonance (CR) transitions. Thus as early as 1939, Mulliken emphasized the existence of CR electronic transitions which are responsible for intense molecular spectra and these have no counterpart in the atomic case [20]. It is these CR transitions which are responsible for large nonperturbative molecule-radiation couplings leading to laser-induced avoided crossings between molecular potentials at moderate intensities [5] and to CREI at current high intensities [10–13,18,19]. As an example, for H_2^+, the first transition moment, $\langle 1\sigma_g|\mathbf{r}|1\sigma_u\rangle = R/2$, leads to a radiative coupling $\mathcal{E}_0 R/2$ between these two molecular orbitals in the presence of a field of maximum amplitude $\mathcal{E}_0$. This coupling displaces the $1\sigma_u$ or LUMO above the internal field + coulomb static barriers for $R < R_c$. For $R > R_c$, the LUMO is trapped below the barriers thus inhibiting the ionization (see [21] for a review of CREI).

The purpose of this work is to extend our previous studies of CREI in linear diatomic molecular systems for the combination of two coherent laser fields with controllable relative intensity and phase between them. Such an approach has triggered a new area of research, coherent control of photochemical and photophysical processes [22] following the pioneering work of Brumer and Shapiro [23]. In the present work we will emphasize the use of symmetry breaking excitation schemes with photons of frequency ω and 2ω and variable relative phase ϕ, for which we have previously shown how to control electron transfer (ET) in photodissociating diatomics [24] and more general ET processes in complex molecules [25]. Thus as illustrated in Fig. 1, varying the relative phase ϕ and relative field amplitude f in the general two field coherent superposition

$$\mathcal{E}(t) = \mathcal{E}_0 [\cos \omega t + f \cos (2\omega t + \phi)] \quad (1)$$

creates a periodic asymmetric field with maximum asymmetry occurring for the parameters $f = 0.5$ and $\phi = 0$. The maximum field amplitude at $\phi = 0$ is then $\mathcal{E}_+ = \mathcal{E}_0 (1 + f)$ corresponding to a maximum intensity $I_+ = I_0 (1 + f)^2$. The minimum amplitude is $\mathcal{E}_- = \mathcal{E}_0 (1 - f)$ with intensity $I_- = I_0 (1 - f)^2$. We have already previously shown that such a periodic asymmetric field (we used $f = 0.25$), will lead to selective ionization at the CREI critical configurations R_c for high intensities, $I = 10^{14}$ W/cm^2, from one atom or the other, in H_2^+ and nonsymmetric H_3^{2+} [26]. We examine in the present work in more detail the feasibility of controlling ionization in molecules with coherent superposition of short intense laser pulses. In particular, we will examine the dependence of this control on the internuclear distance R in addition to discussing the possible application of such laser control of molecular ionization in the current field of laser mass spectrometry [27].

2. Numerical method

Ionization rates are obtained following our previous work by integrating numerically the time-dependent Schroedinger equation (TDSE) on a numerical grid with absorbing boundaries for fixed nuclei, i.e. in the Born-Oppenheimer approximation [10–13]. As an

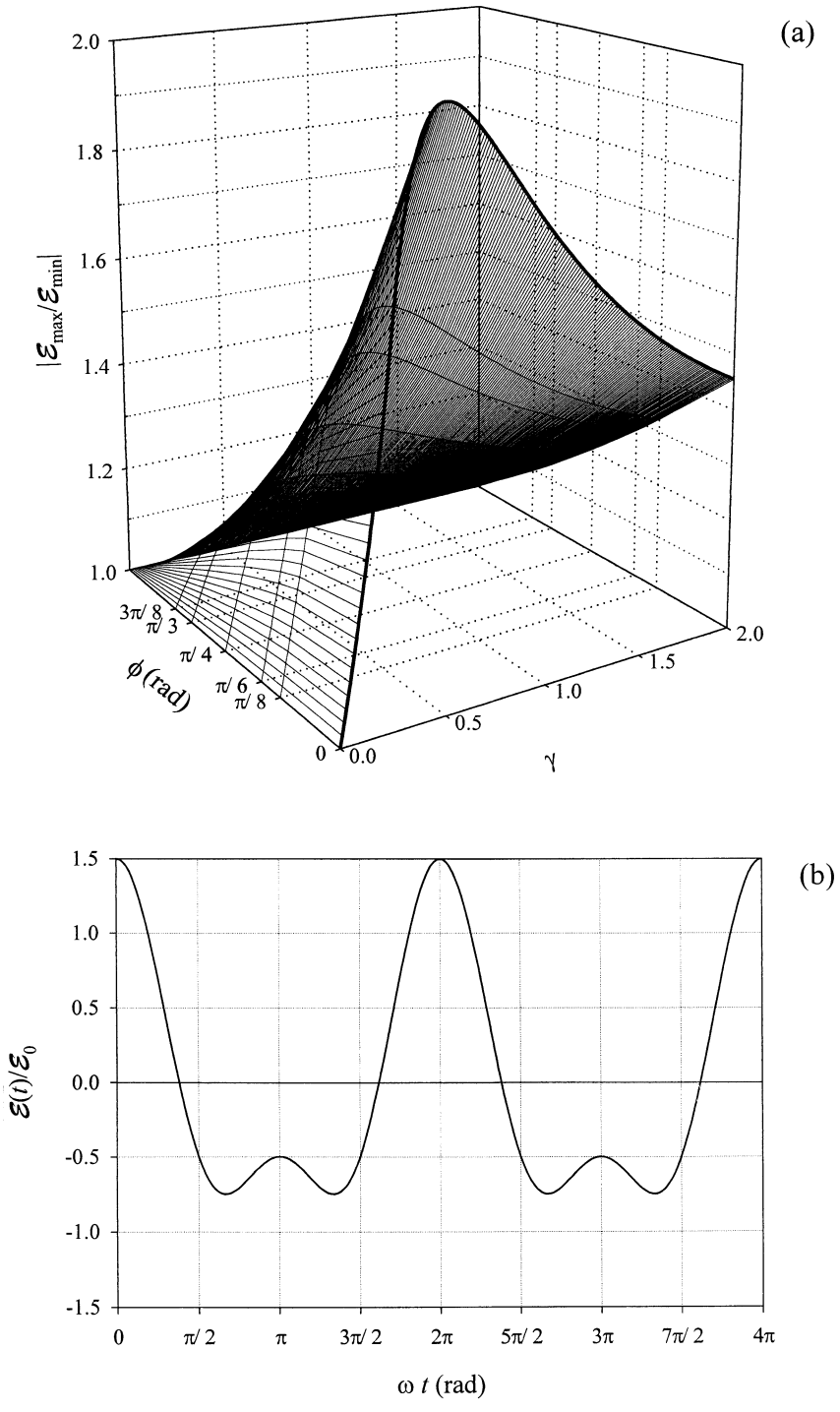

Fig. 1. Total field $\mathcal{E}(t)$, Eq. (1); (a) ratio of maximum $\mathcal{E}_+$, and minimum $\mathcal{E}_-$ amplitudes; (b) profile as a function of phase ωt for $\phi = 0$, $f = 0.5$ parameters.

example, we study first the H_2^+ molecular ion with its molecular orientation parallel to the polarization axis of a linearly polarized ω–2ω laser field combination with the total electric field described by Eq. (1) with relative phase ϕ and relative amplitude f. We choose two values of f, 0.25 and 0.5 with corresponding intensities $I_0 = 0.64$ and 0.44×10^{14} W/cm^2. The net maximum field intensity $I_+ = I_0\ (1 + f)^2$ is then equal to 1×10^{14} W/cm^2 in both cases. Such a choice of intensities is motivated by the fact that one expects ionization to occur at the peak of the fields based upon quasistatic models of multiphoton ionization for atoms [2–4], and for molecules [14,15,18,19]. Thus the above choice of field parameters results in equal maximum intensities $I_+ = 10^{14}$ W/cm^2, for both values of f and we shall explore next the phase sensitivity of such a coherent superposition of fields. We limit ourselves to the wavelength $\lambda = 1064$ nm as in our previous phase control study of molecular ionization [26].

We limit ourselves to one-dimensional (1D) models for one electron H_2^+ and two-electron H_2 molecules. In both cases, we use softened coulomb potentials to remove coulomb singularities [12] allowing us to use efficient split-operator methods [28] to solve the TDSE in the presence of intense laser pulses. For H_2^+ this is written as, (we set $\hbar = m = e = 1$ for atomic units),

$$i\frac{\partial \Psi}{\partial t}(z, R, t) = \left(-\frac{1}{2}\frac{\partial^2}{\partial z^2} + V_c(z, R) + z\mathscr{E}(t)\right)\Psi(z, R, t) \qquad (2)$$

where Ψ is the electronic wave function, z is the electronic coordinate, R the internuclear distance

$$V_c(z, R) = -[c + (z \pm R/2)^2]^{-1/2}, \qquad (3)$$

is the softened coulomb potential and $\mathscr{E}(t)$ is the laser pulse defined in Eq. (1). Choosing $c = 1$ results in a 1D singular free coulomb potential which generally gives good agreement for the ionization potential of the molecular ion with the more accurate 3D calculation [11,12]. The linearly polarized external laser field $\mathscr{E}(t)$ is set parallel to the z, R axis, with a five-cycle ramp time, where it is kept constant during the simulation. An absorbing potential along the electron z direction is used during the propagation of the TDSE(2) by high order split-operator methods [28] to prevent reflection of wave functions at the grid edge. The grid size is chosen to be such that $|z| \leq 512$ a.u. (270 Å). The ionization rates Γ at different internuclear distances R are obtained from the linear time-dependent decrease of the logarithm of the wave function norm [$N(t = 0) = 1$] due to the absorption without reflection after integrating over the electronic z coordinate,

$$\ln N(t) = -\Gamma t, \quad N(t) = \int |\Psi(z, R, t)|^2\, dz \qquad (4)$$

3. Results

Ionization rates calculated from the TDSE for the 1D H_2^+ one electron molecular ion as described in Sec. 2 are illustrated in Fig. 2 for the two phases: (a) $\phi = 0$ and (b) $\phi = \pi/2$. The relative amplitude ratios f are chosen to be (a) $f = 0.25$ for I_0 (10^{14} W/cm^2) = 0.64 and (b) $f = 0.5$ for I_0 (10^{14} W/cm^2) = 0.44. These parameters give a net maximum peak intensity (see Fig. 1) of $I_+ = 10^{14}$ W/cm^2 for both intensities I_0 where maximum ionization is expected to occur. The minimum peak intensities $I_- = I_0\ (1 - f)^2$ can be also obtained from Fig. 1 and these are (a) 3.6×10^{13} W/cm^2 and (b) 1.1×10^{13} W/cm^2, respectively. Fig. 2(a) shows the stability of the CREI critical distance R_c to the two different values of $f = 0.25$ and 0.5 for the ω and 2ω amplitude ratios at the phase $\phi = 0$. This is consistent with the finding that $R_c = 4/I_p \simeq 6$ a.u. as predicted from the CREI theory prediction [16,19] [note: $I_p(H) = 0.67$ a.u. for $c = 1$ in V_c, Eq. (3)]. This theory which is based upon displacement of the LUMO ($1\sigma_u$ in H_2^+) by the CR transition energy $\mathscr{E}_0\ R/2$ or equivalently the static Stark shift of the LUMO predicts R_c values independent of intensity as a result of the nearly equal shift of the LUMO energy and the total internal static field barrier resulting from the peak laser field, $z\mathscr{E}_0$,

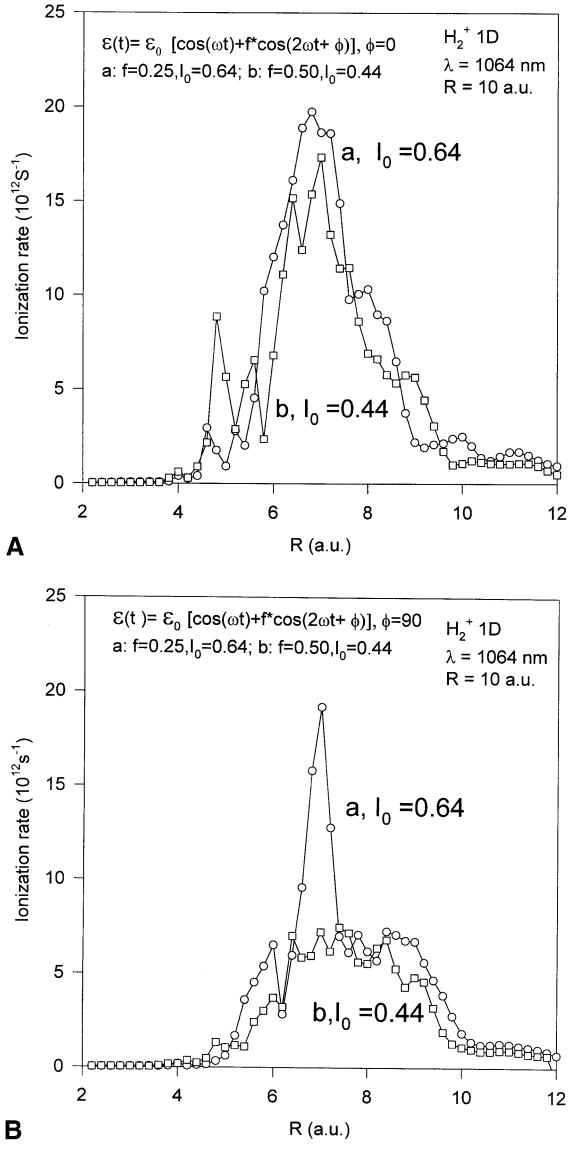

Fig. 2. (a) Ionization rates of H_2^+ at $\lambda = 1064$ nm for field parameters $\phi = 0$ and (a) $f = 0.25$, $I_0 = 0.64$; (b) $f = 0.5$, $I_0 = 0.44$ (10^{14} W/cm^2). (b) Ionization rates of H_2^+ at $\lambda = 1064$ nm for field parameters $\phi = \pi/2$ and (a) $f = 0.25$, $I_0 = 0.64$; (b) $f = 0.5$, $I_0 = 0.44$ (10^{14} W/cm^2).

interaction added to the nuclear coulomb potential V_c. Fig. 2(a) indicates therefore that the ionization occurs mainly at the peak of the field and is controlled by maximum static fields or intensities, $I = 10^{14}$ W/cm^2 in the present case. Fig. 2(b) illustrates the ionization rates obtained for the same field combinations as in Fig. 2(a) but now with the relative phase $\phi = \pi/2$. Such a coherent field superposition gives a symmetric periodic field with equal maxima and minima corresponding to field amplitude ($1.1\mathscr{E}_0$) at $f = 0.25$ and ($1.3\mathscr{E}_0$) at $f = 0.5$. The first field value (a) $f = 0.25$ with intensity $I_0 = 0.64 \times 10^{14}$ W/cm^2 gives a net maximum intensity $I_+ = 8 \times 10^{13}$ W/cm^2 resulting in a similar maximum ionization rate for the same f parameter in Fig. 2(a). The second value, (b) $f = 0.5$ gives the total field ($1.3\mathscr{E}_0$) and since $I_0 = 0.44 \times 10^{14}$ W/cm^2 this gives a slightly lower net intensity of $I = 7 \times 10^{13}$ W/cm^2. The lower ionization rate and a somewhat broader CREI window occurring between 6 and 9 a.u. for the latter is due therefore to the smaller net intensity. In conclusion Fig. 2(a) shows that the field superposition with relative phase $\phi = 0$ maintains the CREI critical distance R_c stable at 7 a.u. with a window $6 < R_c < 8$ a.u., as this is the field superposition with maximum difference between the high and low fields (see Fig. 1). We call this the optimal coherent superposition of the ω and 2ω laser fields. Fig. 3 illustrates in more detail the phase sensitivity of the 1D H_2^+ ionization rates at three different internuclear distances (a) $R = 4$ a.u.; (b) $R = 6$ a.u.; (c) $R = 10$ a.u.. The f and I_0 parameters are again chosen to give the same net maximum intensity $I = 10^{14}$ W/cm^2 as in Fig. 2(a) for combinations giving rise to rates (a) and (b) in each figure. Comparing Fig. 3(a), (b), (c), one notes that one obtains maximum phase sensitivity in the ionization rates to changes in the relative field phase ϕ around the critical distance $R_c = 6$ a.u. Thus at the shorter distance, Fig. 3(a), $R = 4$ a.u., the ionization rates vary by a maximum factor of $\sim$3 when comparing the phase results around $\pi/2$ and π. At the large distance, $R \simeq 10$ a.u., Fig. 3(c), this ratio never exceeds 2. These two internuclear distances correspond to ionization where the CREI mechanism is weakest (see Figs. 2 and 3). Finally, in the CREI region, Fig. 3(b), $R \simeq 6$ a.u., one obtains maximum ionization ratios of nearly one order of magnitude.

The ionization rates at the short distance, $R = 4$ a.u., show broad minima and maxima around $\phi = \pi/2$ and $\phi = 0$, π, respectively. Similar results are

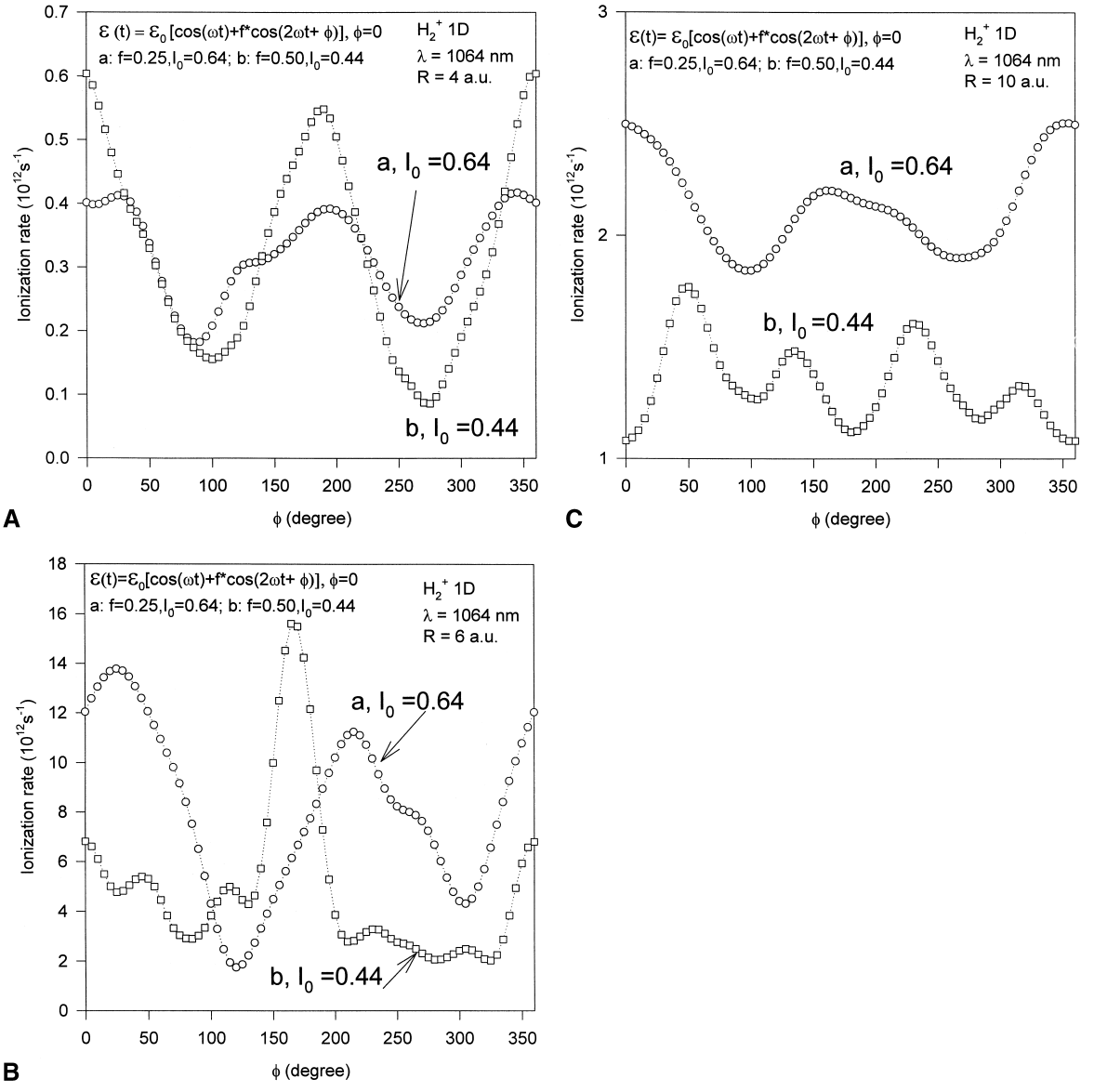

Fig. 3. Ionization rates for H_2^+ at $\lambda = 1064$ nm as a function of field parameters ϕ and $I_0 = 10^{14}$ W/cm^2 for internuclear distances. (a) $R = 4$ a.u.; (b) $R = 6$ a.u.; (c) $R = 10$ a.u.

obtained at distances R, Fig. 3(c), greater than the CREI region. Fig. 3(b) shows that the highest sensitivity occurs for phases $\phi \simeq 0$ or π and amplitude ratios $f = 0.5$, curve (b) with $I_0 = 0.44$ (10^{14} W/cm^2), as seen by the narrow peak around $\phi = \pi$. The ionization rates illustrated in Figs. 2 and 3 and the above discussion lead to the conclusion that the optimal coherent field superposition for controlling ionization rates in H_2^+ occurs for the relative $\phi = 0$ or π and amplitude ratio $f = 0.5$ in ω and 2ω control scenarios. Thus for this optimal pulse condition, most efficient ionization occurs in the CREI region, $R_c \simeq 6$ a.u., as one obtains in this case the largest ionization rates and largest variations of these with ϕ.

We illustrate finally in Fig. 4 the effect of electron correlation on the phase sensitivity of calculated ionization rates of the 1D two electron molecule H_2. As shown in our previous work on H_2, [29], at intensities below 10^{14} W/cm^2 only one electron ionization was obtained from numerical solutions of the corresponding TDSE. In Sec. 2 we concluded that one-electron ionization rates are most sensitive to coherent field phase effects in the CREI region and for the optimal $\omega + 2\omega$ field superposition $\phi = 0$ and $f = 0.5$. Fig. 4 illustrates the effect of two different phases, $\phi = \pi/2$ and 0 on the ionization rate of H_2 as a function of internuclear distance for the above optimal field superposition. Thus at $\phi = 0$, the maximum net intensity is given by $I = 10^{14}$ W/cm^2 whereas at $\phi = \pi/2$, this maximum intensity falls to 7×10^{13} W/cm^2 which explains the lower ionization rate for this case seen in Fig. 4. For the $\phi = 0$ superposition, one obtains maximum sensitivity as manifested by the higher narrower CREI window for $4 < R < 8$ a.u.

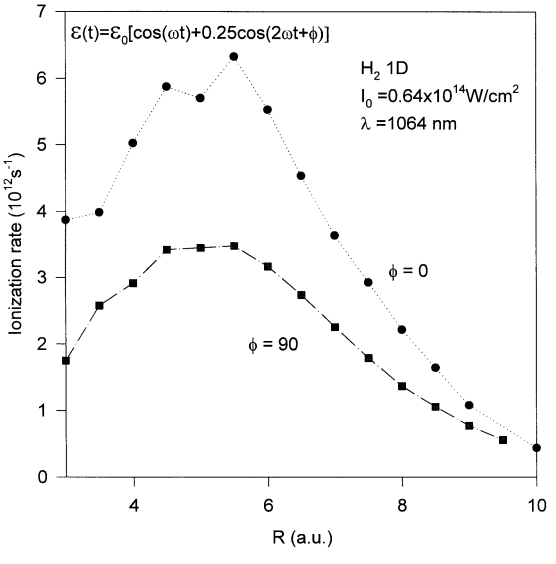

Fig. 4. Ionization rates for H_2 at $\lambda = 1064$ nm as a function of internuclear distance at $\phi = 0$ and 90 and $I_0 = 4.4 \times 10^{13}$ W/cm^2 ($I_0 = c\mathcal{E}_0^2/8\pi$).

4. Conclusion

We have presented highly accurate numerical solutions of the TDSE for the one electron H_2^+ and two electron H_2 molecules in order to investigate possible phase control of ionization in molecules. The present results show that maximum control is achieved for the optimal coherent field superposition of $\omega + 2\omega$ frequencies at relative phase $\phi = 0$ and relative amplitude ratio $f = \mathcal{E}_{2\omega}/\mathcal{E}_{\omega} = 0.5$. This can be readily rationalized from Fig. 1 where it is shown that such parameters give a maximum difference between high $\mathcal{E}_+$ and low $\mathcal{E}_-$ field components of this superposition. The numerical results further show that maximum control is obtained in the CREI region, which occurs at critical internuclear distances R_c for diatomic [18,19] and configurations R_c, θ_c for polyatomics [13]. We have already shown that for H_2^+ [26], ionization occurs mainly from one atom in the CREI region, i.e. the ionization process is localised on one nucleus in this critical region. Furthermore R_c has been shown earlier to be independent of intensity and charge [18,19,21].

Two issues need to be addressed further in order to see whether such laser control of ionization can become useful to laser induced mass spectrometry. The present simulations were performed for static nuclei. We have now extended our numerical method to include nuclear motion in order to simulate real dynamic coulomb explosions [16,17] with applications to laser coulomb explosion imaging (LCEI) [30]. The present static nuclei calculations demonstrate that one should use pulses sufficiently long for the nuclei to reach the critical CREI configurations. Exact dynamic non Born-Oppenheimer calculations will be required to see if the maximum control conditions will remain operative in a real dynamic coulomb explosion experiments. Finally, one can envisage pump–probe experiments, where one initially prepares a molecule into the CREI [11–13] configuration and then one uses the $\omega + 2\omega$ coherent laser pulse superposition to achieve molecular fragmentation by high intensity multiphoton ionization and coulomb explosion. As shown previously, it is the CREI region where the ionization process is localised

to one nucleus [26]. Further simulations and new experiments are therefore required to answer the above questions and thus to establish the present ionization control scheme as a practical scheme for laser control of mass spectrometry.

Acknowledgements

The authors thank NSERC for grants supporting this research; CACPUS for computer time on an IBM-SP2 parallel supercomputer and the following colleagues; S.L. Chin and P.B. Corkum, for useful discussions on multiphoton ionization of molecules.

References

[1] M. Gavrila, Atoms in Intense Laser Fields, Academic, Orlando, FL, 1992.
[2] L. Keldysh, Sov. Phys. JETP 20 (1965) 1307.
[3] P.B. Corkum, N.H. Burnett, F. Brunel, Phys. Rev. Lett. 62 (1989) 1259.
[4] P.B. Corkum, Phys. Rev. Lett. 71 (1993) 1994.
[5] A.D. Bandrauk, Molecules in Laser Fields (Marcel Dekker, New York, 1994).
[6] A.D. Bandrauk, M.L. Sink, Chem. Phys. Lett. 57 (1978) 569; J. Chem. Phys. 74 (1981) 1110.
[7] E. Aubanel, J.M. Gauthier, A.D. Bandrauk, Phys. Rev. A 48 (1993) 2145.
[8] P.H. Bucksbaum, A. Zavriyev, in Molecules in Laser Fields, A.D. Bandrauk (Eds.), Marcel Dekker, New York, 1994, Chap. 2.
[9] C. Wunderlich, H. Figger, T. Hansch, Phys. Rev. Lett. 78 (1997) 2333.
[10] S. Chelkowski, T. Zuo, A.D. Bandrauk, Phys. Rev. A 46 (1992) 5342; 48 (1993) 3837.
[11] T. Zuo, A.D. Bandrauk, Phys. Rev. A 52 (1995) 2511.
[12] H. Yu, A.D. Bandrauk, Phys. Rev. A 56 (1997) 685.
[13] A.D. Bandrauk, J. Ruel, Phys. Rev. A 59 (1999) 2153.
[14] K. Codling, L.J. Frasinski, P.A. Hatherly, J. Phys. B 22 (1989) L321; 26 (1993) 783.
[15] T. Seideman, M.Y. Ivanov, P.B. Corkum, Phys. Rev. Lett. 75 (1995) 2819.
[16] S. Chelkowski, T. Zuo, O. Atabek, A.D. Bandrauk, Phys. Rev. A 52 (1995) 2977.
[17] S. Chelkowski, C. Foisy, A.D. Bandrauk, Phys. Rev. A 54 (1998) 1176.
[18] S. Chelkowski, A.D. Bandrauk, J. Phys. B 28 (1995) L723.
[19] H.T. Yu, T. Zuo, A.D. Bandrauk, J. Phys. B 31 (1998) 1533.
[20] R.S. Mulliken, J. Chem. Phys. 7 (1939) 20.
[21] A.D. Bandrauk, Comments At. Mol. Phys., to be published.
[22] P. Brumer, M. Shapiro, in Molecules in Laser Fields, A.D. Bandrauk (Ed.), Marcel Dekker, New York, 1994, Chap. 6.
[23] P. Brumer, M. Shapiro, Chem. Phys. Lett. 126 (1986) 541.
[24] A.D. Bandrauk, E.E. Aubanel, Chem. Phys. Lett. 229 (1994) 169; Chem. Phys. 198 (1995) 195.
[25] A.D. Bandrauk, H. Yu, in Structure, and Dynamics of Excited States, J. Laane, M. Takahashi, A.D. Bandrauk (Eds.), Springer Verlag, New York, 1998, pp. 177–191.
[26] T. Zuo, A.D. Bandrauk, Phys. Rev. A 54 (1996) 3254.
[27] C. Weickardt, C. Grun, J. Grotemeyer, Eur. Mass. Spectrom. 7 (1999) 257.
[28] A.D. Bandrauk, H. Shen, J. Chem. Phys. 99 (1993) 1185.
[29] H. Yu, A.D. Bandrauk, Phys. Rev. A 54 (1996) 3290.
[30] S. Chelkowski, P.B. Corkum, A.D. Bandrauk, Phys. Rev. Lett. 82 (1999) 3416.